Molecular Crystals and Liquid Crystals

Publication details, including instructions for authors and subscription information:
http://www.tandfonline.com/loi/gmcl20

Rheological Response of Polydisperse Nematic Polymethacrylates: Relaxation Times and Conformational Transition

Laura Andreozzi [a], Massimo Faetti [a], Fabio Zulli [a], Marco Giordano [a] & Giancarlo Galli [b]

[a] Dipartimento di Fisica "E. Fermi,", Università di Pisa and INFM, Pisa, Italy

[b] Dipartimento di Chimica e Chimica Industriale, Università di Pisa and INSTM, Pisa, Italy

Version of record first published: 17 Oct 2011

To cite this article: Laura Andreozzi, Massimo Faetti, Fabio Zulli, Marco Giordano & Giancarlo Galli (2005): Rheological Response of Polydisperse Nematic Polymethacrylates: Relaxation Times and Conformational Transition, Molecular Crystals and Liquid Crystals, 441:1, 13-26

To link to this article: http://dx.doi.org/10.1080/154214091009518

Mol. Cryst. Liq. Cryst., Vol. 441, pp. 13–26, 2005

ISSN: 1542-1406 print/1563-5287 online
DOI: 10.1080/154214091009518

Taylor & Francis
Taylor & Francis Group

Rheological Response of Polydisperse Nematic Polymethacrylates: Relaxation Times and Conformational Transition

Laura Andreozzi
Massimo Faetti
Fabio Zulli
Marco Giordano
Dipartimento di Fisica "E. Fermi," Università di Pisa and INFM, Pisa, Italy

Giancarlo Galli
Dipartimento di Chimica e Chimica Industriale, Università di Pisa and INSTM, Pisa, Italy

We investigated the rheological behavior of two nematic polymethacrylate homopolymer samples, S1 and S5, containing azobenzene side groups. They possessed different molar mass and molar mass distribution, which was fitted by a two-component molar mass distribution function. Creep and oscillatory measurements enabled us to obtain the temperature dependence of the zero shear viscosity. The time-temperature superposition principle was found to hold over large temperature intervals; in particular no discontinuities were detected at the isotropic–nematic transition in either sample. Moreover, temperature scans of the storage modulus of the polymers at a constant frequency were marked by glass and conformational transitions, the conformation transition being driven by the nematic order. The storage modulus and the distribution of relaxation times were analyzed in terms of the two components of the molar mass distribution.

Keywords: conformational transition; nematic polymer; rheology; TTS

INTRODUCTION

In the last years, liquid crystalline polymers containing azobenzene side groups have been deeply investigated because of their potential

Address correspondence to Laura Andreozzi, Dipartimento di Fisica "E. Fermi," Università di Pisa and INFM, via F. Buonarroti 2, Pisa 56127, Italy. E-mail: laura.andreozzi@df.unipi.it

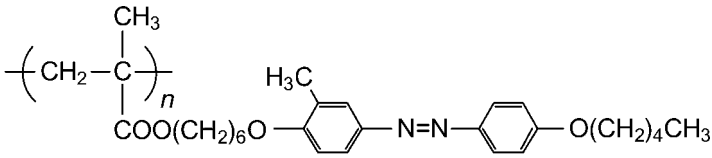

FIGURE 1 The structure of the nematic PMA4 homopolymers S1 and S5.

application as media in photonics and optoelectronics [1–3], and especially they have proven to be suitable candidates for optical information storage [1,2]. We accomplished in fact optical writing at both micrometer and nanometer length scales in the nematic polymethacrylate PMA4 system, homopolymers and copolymers, that consists of a suitably substituted and spaced azobenzene side group [4–7] (Fig. 1). Variations of the molar mass and molar mass distribution in the homopolymers and of the chemical composition of the copolymers (with methyl methacrylate) allowed the transition temperatures of the PMA4 samples to be tuned. This in turn resulted in the possibility of storing optical data under varied experimental conditions.

Bit stability, homogeneity at molecular level, and working temperature range are crucial materials parameters to achieve an effective, high-resolution and long-term data storage [4,5]. Therefore, techniques that cover different time and length scales must be employed in order to fully characterize the polymer matrices of interest.

In the present work, we extended our rheological investigations of dynamic shear and creep behaviors to cover the whole temperature range from the isotropic melt, across the nematic phase, down to the glassy state of two PMA4 homopolymer samples S1 and S5 having different molar mass and molar mass distribution. The time-temperature superposition (TTS) principle was found to hold through the whole investigated temperature range, even across the nematic–isotropic transition in both samples, and effects of the molar mass distributions on relaxation times were pointed out. Signatures of glass and conformation transitions were detected in the storage modulus G' and are discussed in terms of the molar mass composition of the homopolymers S1 and S5.

MATERIALS AND EXPERIMENTAL

The PMA4 S1 and S5 homopolymer samples were prepared by free-radical polymerization according to a literature procedure [8]. Their physico-chemical and thermal characteristics are reported in Table 1.

TABLE 1 Physico-Chemical and Thermal Characteristics of the PMA4 Homopolymer Samples S1 and S5

Sample	M_n (g/mol)	M_w (g/mol)	M_z (g/mol)	M_w/M_n	T_g (K)	T_c (K)	T_{NI} (K)
S1	18600	59000	171200	3.17	292	320	353
S5	29900	72600	130500	2.43	305	337	357

Average molar masses (M_n, M_w, M_z) were determined by size exclusion chromatography (SEC) on chloroform solutions with a 590 Waters chromatograph that was equipped with two Shodex KF804 columns and both RI R401 and UV LC75 detectors. Polystyrene standard samples ($M_n = 1{\cdot}10^3$–$5{\cdot}10^5$ g/mol) were used for the calibration.

Careful studies carried out to reproduce numerically the experimental molar mass distribution of PMA4 samples showed [9] that the logarithmic normal (LN) function represents their molar mass distribution better than Zimm-Schulz (ZS) functions [10]. The LN function, written as

$$W_{LN}(M,\bar{M},\sigma) = \frac{1}{\sqrt{2\pi\sigma^2}} \cdot \frac{1}{M} \cdot \exp\left[-\frac{(\ln M - \ln \bar{M})^2}{2\sigma^2}\right] \tag{1}$$

is a function of the molar mass M, the average molar mass $\bar{M}$, and the standard deviation σ. At the lowest order of approximation, experimental chromatograms W_{EXP} can be expanded as superpositions of two distributions:

$$W_{EXP}(M) = A_1 \cdot W_{LN}(M,\ \bar{M}_1,\ \sigma_1) + A_2 \cdot W_{LN}(M,\ \bar{M}_2,\ \sigma_2) \tag{2}$$

The A_1 and A_2 fit parameters of Eq. (2) together with the number-average and the weight-average molar masses and the polydispersity indices for the i-th component W_{LN} of the W_{EXP} are reported in Table 2.

TABLE 2 Parameters of the Molar Mass Distribution Obtained by Using Two LN Functions

Sample	A_1	M_{n1} (g/mol)	M_{w1} (g/mol)	M_{w1}/M_{n1}	A_2	M_{n2} (g/mol)	M_{w2} (g/mol)	M_{w2}/M_{n2}
S1	0.16	42700	48700	1.14	0.84	16700	25200	1.51
S5	0.56	71800	107000	1.49	0.44	16900	31200	1.85

Differential scanning calorimetry (DSC) measurements were performed with a Perkin-Elmer DSC7 calorimeter (10 K/min scanning rate) calibrated with indium and zinc standards.

Rheological measurements, both continuous and oscillatory, were carried out with a Haake RheoStress RS150H rheometer in the plane-plate geometry (20 mm diameter) in the temperature range 303–413 K under highly pure nitrogen flow. In order to account for thermal dilatation of the system, the gap in the plane parallel geometry was automatically varied in the temperature range between 0.40 μm and 0.60 μm. The gap was chosen significantly larger than the polymer chain length to permit gap independent measurements. The sample temperature was stable within 0.1 K.

To ensure that all measurements were carried out in the linear regime, preliminary tests on viscoelastic linearity of the materials were conducted. Zero shear viscosity η was obtained in two independent ways by i) creep measurements at different temperatures, and ii) loss modulus G'' resulting from frequency sweep measurements.

RESULTS AND DISCUSSION

We investigated the rheological properties of two PMA4 homopolymer samples, S1 and S5, having different molar mass and molar mass distribution (Table 1). This was fitted by superposing two logarithmic normal functions (Fig. 2). The corresponding high molar mass and low molar mass components will be labeled herein as 1 and 2, respectively. Both homopolymers S1 and S5 evidenced a change in heat

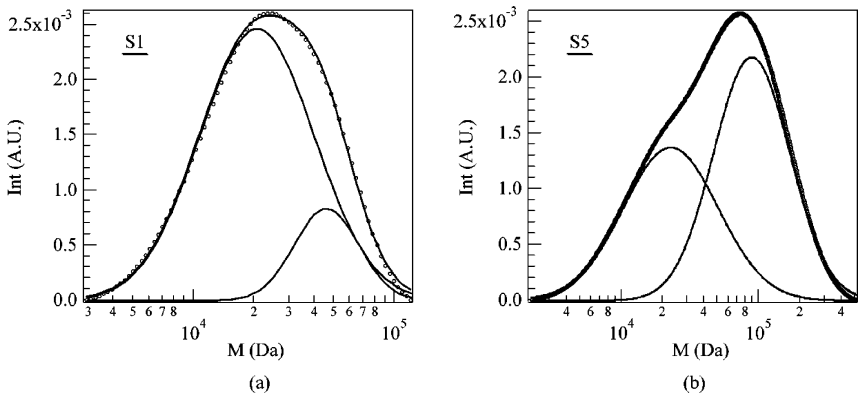

FIGURE 2 SEC curves and best fits with two LN functions for S1 (a) and S5 (b).

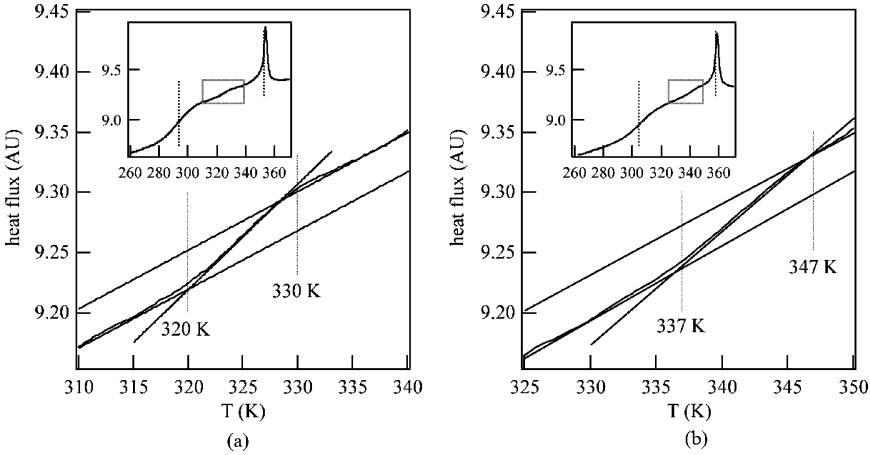

FIGURE 3 DSC heating scans for S1 (a) and S5 (b), with the enlarged 310–340 K and 325–350 K regions (10 K/min heating rate).

capacity associated with a conformational transition at the onset temperature T_c of 320 K and 337 K, respectively, [9] (Fig. 3) in addition to the glass transition temperature T_g and the nematic–isotropic temperature T_{NI} (Table 1).

Time Temperature Superposition Principle and Relaxation Time Distributions

The rheological measurements were performed in the temperature ranges of 303–403 K and 313–413 K for S1 and S5, respectively. The values of their viscosity obtained in independent ways by oscillatory measurements, $\eta = \lim_{\omega \to 0}(G''/\omega)$, and creep measurements are collected and plotted vs. $1000/T$ in Figure 4. No discontinuity of the viscosity was observed at the T_{NI} in either sample. The viscosity data were found to follow a Vogel-Fulcher law (VF):

$$\eta(T) = \eta_\infty \exp\left(\frac{T_b}{T - T_0}\right) \tag{3}$$

The values found for the pseudo-activation energy T_b, the Vogel temperature T_0, and η_∞ are given in Table 3. They are typical of side group polymers, the value of T_b depending on the stiffness of the polymer backbone.

As is shown in Figure 5, both homopolymers showed superimposable storage G' and loss G'' moduli in the nematic and isotropic phases,

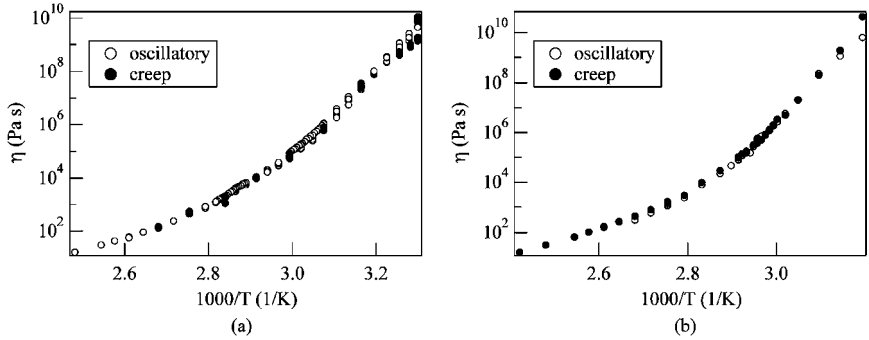

FIGURE 4 Zero-shear viscosity data from creep (bullets) and oscillatory (circles) measurements for S1 (a) and S5 (b).

and also across the conformation transition temperature. This finding and the fact that viscosity data from oscillatory and creep measurements were well superimposable (Fig. 4) confirm that the TTS principle also holds for these side group polymers. In fact, previous results on similar liquid crystal polymers [11,12] showed a failure of TTS only for samples with very high molar masses [11].

According to the TTS principle, the dependence of the shear elastic complex modulus on ω and T can be written as a function of the shear elastic complex modulus measured at the reference temperature T_r [13]:

$$G^*(\omega T) = b_{Tr}(T)G^*(a_{Tr}(T)\omega T_r). \tag{4}$$

The vertical and horizontal shift parameters, $b_{Tr}(T)$ and $a_{Tr}(T)$, are two real temperature-dependent functions. The $a_{Tr}(T)$ factor strongly depends on temperature and follows the Williams-Landel-Ferry law (WLF) [13]:

$$-\log a_{T_r}(T) = \frac{C_1(T - T_r)}{C_2 + T - T_r} \tag{5}$$

A mathematical shift of the experimental isothermal frequency sweeps of $G^*(\omega)$ [14] leads to the calculation of master curves and of horizontal

TABLE 3 VF Best-fit Parameters

Sample	T_b (K)	T_0 (K)	η_∞ (Pa·s)
S1	1300 ± 30	259 ± 5	$(2.12 \pm 0.03) \cdot 10^{-3}$
S5	1100 ± 30	278 ± 3	$(3.70 \pm 0.05) \cdot 10^{-3}$

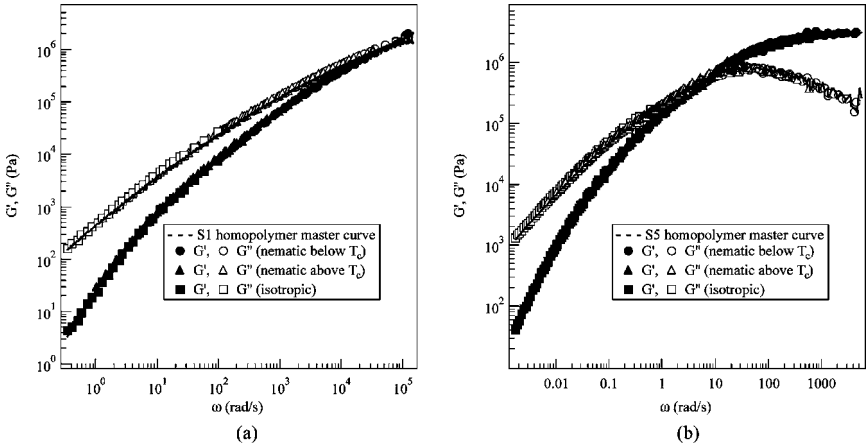

FIGURE 5 Superimposed master curves for S1 (a) and S5 (b), at various reference temperatures in different phases: isotropic (squares), nematic above T_c (triangles), nematic below T_c (circles).

and vertical shift factors at the reference temperature. The WLF parameters C_1 and C_2 at T_r obtained from fitting the $a_{Tr}(T)$ for S1 and S5 samples with Eq. 5, are given in Table 4. According to TTS and Doolittle equation, the relations $T_0 = T_r - C_2$ and $T_b = C_1C_2 \cdot \ln 10$ can be found between the VF and WLF parameters [13]. Fit parameters of S1 and S5 confirmed these relations within the experimental error (Tables 3 and 4). Moreover, being C_1C_2 and $T_r - C_2$ constants independent of T_r, it is also possible to remove any further dependence on polymer chain mobility in C_1 and C_2 extrapolating the WLF parameters at T_g: C_1^g and C_2^g [15]. Nearly coincident C_1^g and C_2^g were found for PMA4 samples providing a confirmation that their rheological properties are dominated by the polymer backbone [11].

Figure 6 illustrates the master curves of S1 and S5 with reference temperatures at the same T_r/T_g ratio ($T_r = 322\,\mathrm{K}$ for S1, and $T_r = 338\,\mathrm{K}$ for S5). In both master curves, a liquid behavior is observed in the low frequency side. In particular, the S5 sample shows the flow

TABLE 4 WLF Best-fit Parameters at the Reference Temperature T_r and Invariants

Sample	C_1	C_2 (K)	T_r (K)	$C_1C_2 \cdot \ln 10$ (K)	$T_r - C_2$ (K)	C_1^g	C_2^g (K)
S1	9.2 ± 0.1	60 ± 1	322.0 ± 0.1	1270 ± 40	262 ± 1	18 ± 2	30 ± 2
S5	8.0 ± 0.1	60 ± 1	338.0 ± 0.1	1100 ± 30	278 ± 1	18 ± 1	27 ± 2

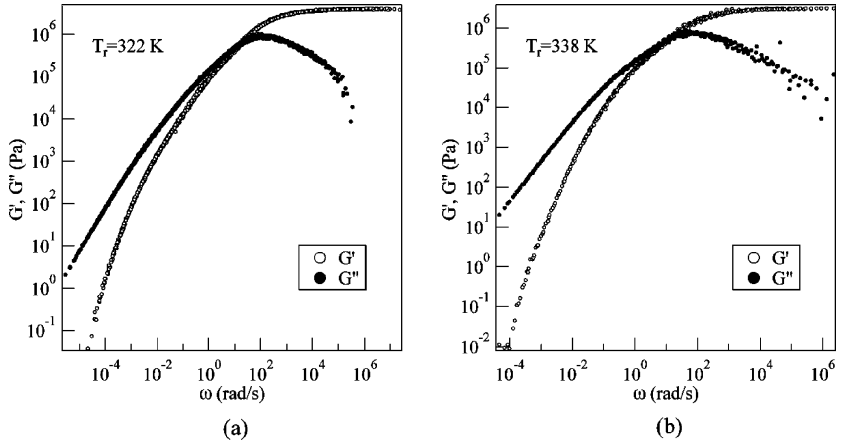

FIGURE 6 Master curves of storage (empty circles) and loss moduli (filled circles) for S1 at $T_r = 322\,\mathrm{K}$ (a) and S5 at $T_r = 338\,\mathrm{K}$ (b).

region at lower frequencies with respect to S1, the high molar mass component 1 rising the terminal time. No evidence of a rubbery plateau characteristic of entanglement effects can be observed. Entanglement could have been anticipated especially in S5, as in various acrylic polymers such a plateau first appears roughly at the critical molar mass $M_c' \sim 3M_e \sim 24000\,\mathrm{g/mol}$ [16], with M_e the entanglement molar mass. However the absence of entanglement was also inferred from the master curves of several analogous azobenzene polymethacrylates [12], even at molar masses expected to be above M_c'. The lack of a plateau could be due to the nematic order that dilates the confining tube of the polymer, on which dimension the M_e value depends [16], and shifts entanglement to higher molar masses.

From the master curves of S1 and S5, the relaxation time distribution $\rho(\tau, T_r)$ was calculated with a nonlinear regularization method [17]. In fact, the relaxation of a real viscoelastic material is ruled by the law for the complex modulus $G^*(\omega)$ in the frequency regime at the reference temperature [17]:

$$G^* = G_\infty \int_{-\infty}^{+\infty} \frac{\omega^2\tau^2 + i\omega\tau}{1 + \omega^2\tau^2} \rho(\tau) d(\ln \tau) \tag{6}$$

where ρ, ω, τ, and G_∞ are real valued. The relaxation times τ are supposed to follow the same temperature dependence as for η [13]:

$$\tau(T) = \tau_\infty \exp\left(\frac{T_b}{T - T_0}\right). \tag{7}$$

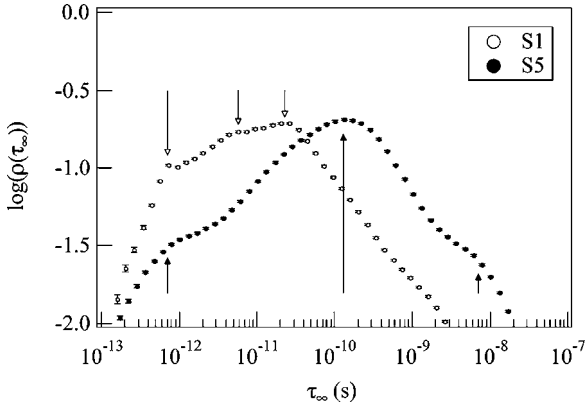

FIGURE 7 Relaxation time distributions $\rho(\tau_\infty, T_r)$ for S1 (empty circles) and S5 (filled circles) (arrows point to: S1 τ_∞^{st}, τ_∞^{R1} and τ_∞^{R2}; S5 τ_∞^{st}, τ_∞^{R1} and τ_∞^{d1}).

In Figure 7 are reported the curves $\rho(\tau_\infty,\ T_r)$ of the relaxation time distributions for S1 and S5 in an iso-frictional state. The structural τ_∞^{st}, the Rouse τ_∞^{R1} and τ_∞^{R2}, and the disengagement τ_∞^{d1} relaxation times are also marked in Figure 7 and reported in Table 5. The structural times resulted to have the same value $\tau_\infty^{st} = (7.0 \pm 0.8)\cdot 10^{-13}$ for both S1 and S5 samples, as expected. It is worth noting that the ratio between all the Rouse times follows a square dependence on M_w. The Rouse time pertinent to the low molar mass component of S5 sample was not detected because the high molar mass component 1 gives a overwhelming contribution to the relaxation time distribution.

Conformational Transition

Previous ESR and LODESR studies of the homopolymer dynamics suggested [5,7] that, on lowering temperature, a conformational transition of the polymer backbone took place in the 320–340 K temperature range, driven by the increasing nematic order in the side groups. As a consequence of the conformational transition, an increase in the polymer main chain stiffness is expected at lower temperatures than T_c.

TABLE 5 Structural τ_∞^{st}, Rouse τ_∞^{R1} and τ_∞^{R2} (Highest 1 and Lowest 2 Component), and Disengagement τ_∞^{d1} Relaxation Times Evaluated from Figure 7

Sample	M_{w1} (g/mol)	M_{w2} (g/mol)	τ_∞^{st} (ps)	τ_∞^{R1} (ps)	τ_∞^{R2} (ps)	τ_∞^{d1} (ps)
S1	48700	25200	0.7	25	5.7	–
S5	107000	31200	0.7	130	–	6000

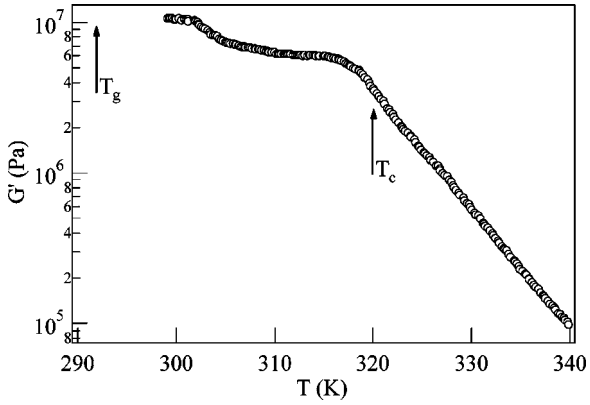

FIGURE 8 Temperature scan of storage modulus at the frequency of 10 Hz for S1. Arrows point to DSC transition temperatures.

Evidence that the polymer is more rigid below T_c is provided by the data shown in Figure 8, which illustrates an oscillatory temperature scan for S1. The trend of G' with temperature, at the fixed frequency of 10 Hz, clearly shows a plateau at ca. 10^7 Pa up to T_g and a second plateau at ca. $6{\cdot}10^6$ Pa up to approximately T_c. A pronounced drop in modulus is then detected as the temperature is increased in the nematic phase. The 10 Hz measurements are on a fast time scale with respect to the polymer dynamics around the T_g, and the glassy plateau lasts for several degrees above the glass transition temperature determined by DSC measurements. However, in the vicinity of the

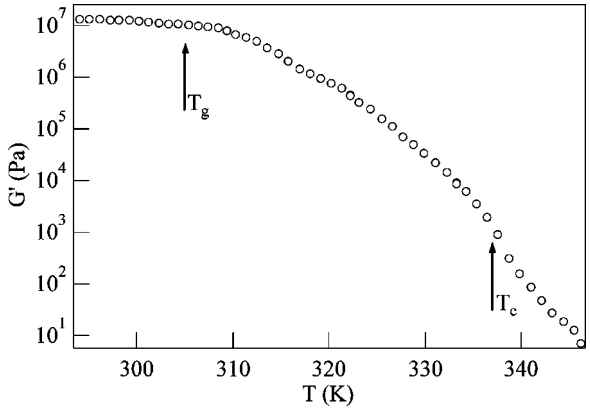

FIGURE 9 Temperature scan of storage modulus at the frequency of 0.00147 Hz for S5. Arrows point to DSC transition temperatures.

T_c the polymer dynamics is fast enough with respect to 10 Hz oscillatory measurements and the conformational crossover is signaled more precisely.

A different behavior can be observed for S5 inFigure 9, where a temperature scan of G′ at the frequency of 0.00147 Hz is reported. Here, both T_g and T_c can be detected as changes in the slope of the G′ curve. The larger content of the high molar mass component in S5 explains the lack of the conformational plateau.

To gain further insight, we deconvolved the G′ curve for S5 in two curves pertinent to the two components of molar mass distribution. A trial function could be obtained starting from a series of Debye-like contributions [14] in terms of T_g and T_c of the i-th component

$$G'(T) = \sum_{\substack{i=1,2 \\ T_j = T_g,\, T_c}} G_\infty^{(i)}(T_j^{(i)}) \frac{\omega^2 \tau^2(T; T_j^{(i)})}{1 + \omega^2 \tau^2(T;\ T_j^{(i)})} \theta(T_j^{(i)} - T),$$

where

$$\theta\,(T_j^{(i)} - T) = \begin{cases} 1 \Leftarrow T \leq T_j^{(i)} \\ 0 \Leftarrow T > T_j^{(i)} \end{cases}. \tag{8}$$

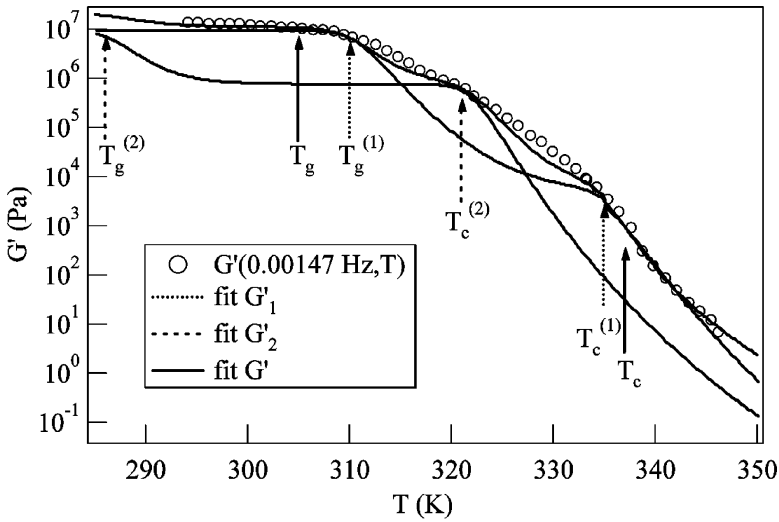

FIGURE 10 Temperature scan of storage modulus at the frequency of 0.00147 Hz for S5 with superimposed fitting curves of components 1 and 2, and their sum.

Because for TTS $\tau(T) = a_{T_r}(T)\tau(T_r)$, being $\omega\tau(T_j^{(i)}; T_j^{(i)}) = 1$, from Eq. (8) one writes

$$G'(T) = \sum_{\substack{i=1,2 \\ T_j = T_g, T_c}} G_\infty^{(i)}(T_j^{(i)}) \left(\frac{a^2_{T_j^{(i)}}(T)}{1 + a^2_{T_j^{(i)}}(T)} \right)^{\beta_{T_j^{(i)}}} \theta(T_j^{(i)} - T) \tag{9}$$

in which we introduced the β-power dependence to approximate more precisely the slope of the $G'(T)$ curve. Figure 10 shows experimental and theoretical curves from Eq. (9), the parameters of which are given in Table 6. The glass transition temperatures $T_g^{(1)}$ and $T_g^{(2)}$ were chosen according to the Fox-Flory relationship:

$$T_g(M_n) = T_g^{(\infty)} - \frac{K_n}{M_n} \tag{10}$$

in which both parameter $K_n = 878200\,\mathrm{K \cdot g/mol}$ and glass transition temperature at infinite molar mass $T_g^{\infty} = 324\,\mathrm{K}$ werepreviously found for PMA4 homopolymers [9]. The temperatures $T_c^{(1)}$ and $T_c^{(2)}$ were obtained as free parameters from the best fit of the overall G' profile. Note that the critical temperature of the low molar mass component 2 of S5, $T_c^{(2)}$, fairly agrees with the one of S1. Also, the plateau regime and the overall shape of $G'(T)$ for S1 and the low molar mass component 2 of S5 are nicely parallel. This is consistent with their almost identical values of $\mathrm{M_n}$. Moreover, the $G'_\infty(\mathrm{T_g})$ values are typical for polymers, while the $G'_\infty(\mathrm{T_c})$ values pertinent to the conformational transitions are allowed to assume any value with the only physical constraint of good reproduction of the G′ curve in the region of the conformational transition.

Moreover, as already stressed, the ratio $G'_\infty(T_g)/G'_\infty\ (T_c)$ is about 2 for S1. A plateau regime is also exhibited by the low molar mass component 2 of S5, being $G'_\infty(T_g^{(2)})/G'_\infty(T_c^{(2)})$ about 10. On the other hand, component 1 evidences the presence of $T_c^{(1)}$, but does not show the plateau being $G'_\infty(T_g^{(1)})/G'_\infty(T_c^{(1)})$ about 2500.

TABLE 6 Parameters of Eq. (9) adopted in Simulating the Temperature Scan G' (T, 0.00147 Hz) for S5 (Fig. 10)

S5 component (i)	$G'_\infty(T_g^{(i)})$ (Pa)	$T_g^{(i)}$ (K)	$\beta_{T_g}^{(i)}$	$G'_\infty(T_c^{(i)})$ (Pa)	$T_c^{(i)}$ (K)	$\beta_{T_c}^{(i)}$
Highest (1)	$1{\cdot}10^7$	310	0.25	$4{\cdot}10^3$	335	1.0
Lowest (2)	$1{\cdot}10^7$	287	0.25	$9{\cdot}10^5$	322	0.65

CONCLUSIONS

The rheological properties of two different samples of PMA4 homopolymers (S1 and S5) with low and high molar mass components were compared. In particular, the TTS principle holds in these polymers, even across the transition temperatures, which provides further evidence of the role of the main chain in dictating the relaxational dynamics.

We also found that rheometry is able to detect glass and conformation transitions. The two samples showed varied temperature scans of storage modulus. While S1 presents a plateau between T_g and T_c, S5 does not show this conformational plateau. This behavior is attributed to the different distributions of molar mass components of the polymer samples, each of them exhibiting distinct T_g and T_c values. Such conformational transitions in turn are of special relevance as they stabilize optical information stored in the polymer matrix below T_c.

REFERENCES

[1] For a review, see Natansohn, A. & Rochon, P. (2002). *Chem. Rev.*, *102*, 4139.
[2] (a) Yaroshchuk, O., Bidna, T., Dumont, M., & Lindau, J. (2004). *Mol. Cryst. Liq. Cryst.*, *409*, 229.
(b) Nakano, M., Yu, Y., Shishido, A., Tsutsumi, O., Kanazawa, A., Shiono, T., & Ikeda, T. (2003). *Mol. Cryst. Liq. Cryst.*, *398*, 1.
(c) Wuestneck, R., Stumpe, J., Karageorgieva, V., Meier, L. G., Rutloh, M., & Presher, D. (2002). *Coll. Surf. Physicochem. Engineer. Asp.*, 198–200, 753.
(d) Bubliz, D., Helgert, M., Fleck, B., Wenke, L., Hvilsted, S., & Ramanujam, P. S. (2000). *Appl. Phys. B*, *70*, 803.
[3] Villacampa, B., Sanchez, C., Rodriguez-Martinez, F. J., Cases, R., Alcalá, R., Oriol, L., Millaruelo, M. (2004). *Mol. Cryst. Liq. Cryst.*, *411*, 467.q
[4] Andreozzi, L., Faetti, M., Galli, G., Giordano, M., & Palazzuoli, D. (2004). *Macromol. Symp.*, *218*, 323, and references therein.
[5] Andreozzi, L., Faetti, M., Galli, G., Giordano, M., & Palazzuoli, D. (2001). *Macromolecules*, *34*, 7325.
[6] Likodimos, V., Labardi, M., Pardi, L., Allegrini, M., Giordano, M., Arena, A., & Patanè, S. (2003). *Appl. Phys. Lett.*, *82*, 3313.
[7] Andreozzi, L., Bagnoli, M., Faetti, M., & Giordano, M. (2001). *Mol. Cryst. Liq. Cryst.*, *372*, 1.
[8] Angeloni, A. S., Caretti, D., Laus, M., Chiellini, E., & Galli G. (1991). *J. Polym. Sci., Polym. Chem. Ed.*, *29*, 1865.
[9] Andreozzi, L., Faetti, M., Giordano, M., Palazzuoli, D., Laus, M., & Galli, G. (2003). *Mol. Cryst. Liq. Cryst.*, *398*, 97.
[10] Brandrup, J. & Immergut, E. H. (Eds.), (1989). *Polymer Handbook*, 3rd ed., John Wiley & Sons, New York.
[11] Berghausen, J., Fuchs, J. & Richtering, W. (1997). *Macromolecules*, *30*, 7574.
[12] Colby, R. H., Gillmor, J. R., Galli, G., Laus, M., Ober, C. K. & Hall, E. (1993). *Liq. Cryst.*, *13*, 233.
[13] Ferry, J. D. (1980). *Viscoelastic Properties of Polymers*, Wiley: New York.

[14] Honerkamp, J. & Weese, J. (1993). *Rheol. Acta*, *32*, 57.
[15] Fuchs K., Friedrich C., & Weese J. (1996). *Macromolecules*, *29*, 5893.
[16] Fetters L. J., Lohse D. J., Richter, D., Witten, T. A., & Zirkel A. (1994). *Macromolecules*, *27*, 4639.
[17] (a) Honerkamp, J. & Weese, J. (1993). *Rheol. Acta*, *32*, 65.
(b) Weese, J. (1993). *J. Comput. Phys. Commun*., *77*, 429.